Electron-Transfer Chemistry of the Iron–Molybdenum Cofactor of Nitrogenase: Delocalized and Localized Reduced States of FeMoco which Allow Binding of Carbon Monoxide to Iron and Molybdenum

Christopher J. Pickett,*[a] Kylie A. Vincent,[b] Saad K. Ibrahim,[a] Carol A. Gormal,[a] Barry E. Smith,[a] and Stephen P. Best*[b]

Abstract: The electron-transfer chemistry of the isolated iron–molybdenum cofactor of nitrogenase (FeMoco) has been studied by electrochemical and spectroelectrochemical methods. Two interconverting forms of the cofactor arise from a redox-linked ligand isomerism at the terminal iron atom; this is attributed to rotamerism of an anionic *N*-methyl formamide ligand bound at this site. FeMoco in its EPR-silent oxidised state is shown to undergo three successive one-electron transfer steps. We argue that the first and second redox processes are associated with electron-transfer delocalised over the iron–sulfur core of the cofactor, whilst the third irreversible process is localised on molybdenum. This is strongly reinforced by spectroelectrochemical studies under ^{12}CO and ^{13}CO which reveal two independent carbon monoxide binding sites that are specifically associated with the second (iron core) and third (molybdenum) electron-transfer processes and which give rise to terminal $\nu(^{12}CO)$ bands at 1885 and 1920 cm^{-1} respectively. Moreover, in parallel with earlier studies on the enzyme system, it is shown that at low CO concentration, carbon monoxide binds to the cofactor in bridging modes, with $\nu(CO)$ bands at 1835 and 1808 cm^{-1} that are interconverted by single-electron transfer. Importantly we show that the contentious overall 2e difference in the assignment of the metal oxidation levels in the resting state of the enzyme-bound cofactor, arising from analysis of ^{57}Fe ENDOR and Mössbauer data, can be resolved in the light of the electron-transfer chemistry of the isolated cofactor described herein.

Keywords: bridging ligands · cofactors · electrochemistry · IR spectroscopy · nitrogen fixation · nitrogenases

Introduction

Integration of substrate binding with electron and proton transfer at an $\{Fe_7S_9Mo\}$ cluster confined within a protein is the essence of a key biological process, nitrogen fixation.[1] The structure of this cluster (the M centre) within the crystalline resting-state nitrogenase MoFe protein has been established by Rees and co-workers and is represented in Figure 1.[2] However, the site and mode of binding of molecular nitrogen to the cluster and the mechanism of its subsequent reduction to ammonia are unknown. Consequently, there has been considerable scope for speculation on how nitrogenase works with diverse mechanisms postulated from chemical and theoretical studies on model[3, 4] and in silico[5] systems. A very recent high-resolution structure of the MoFe protein of nitrogenase from *Azotobacter vinelandii* has led to a revision of the nature of the M centre: it is suggested that an interstitial N atom (or possibly C or O) is contained within the central 6Fe3S cavity, octahedrally coordinated by the Fe atoms. The presence of this light atom clearly disposes of the peculiar unsaturation of the six "trigonal" iron atoms and is most likely a structural element cross-linking the atoms of the

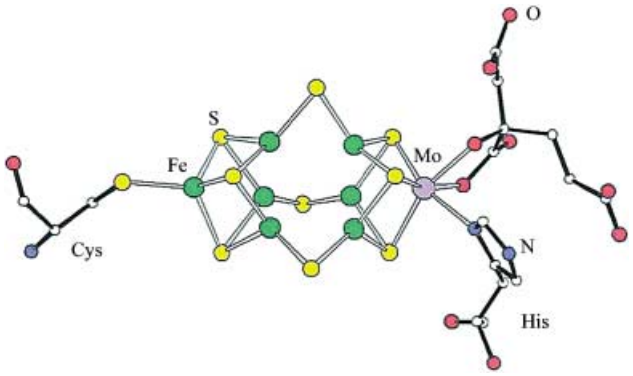

Figure 1. View of the M centre in the MoFe protein of *A. vinelandii* nitrogenase from X-ray crystallographic data of Rees et al. as first reported in 1992.[2]

[a] Prof. C. J. Pickett, Dr. S. K. Ibrahim, C. A. Gormal, Prof. B. E. Smith
Department of Biological Chemistry, John Innes Centre
Norwich, NR4 7UH (UK)
Fax: (+44) 1603-450018
E-mail: chris.pickett@bbsrc.ac.uk

[b] Dr. S. P. Best, K. A. Vincent
School of Chemistry, University of Melbourne
Victoria 3010 (Australia)
Fax: (+61) 39347-5180
E-mail: spbest@unimelb.edu.au

0947-6539/03/0901-0076 $ 20.00+.50/0 *Chem. Eur. J.* **2003**, *9*, No. 1

trigonal prism to give a robust structure.[6] Key questions such as the oxidation states of the metal atoms in the cluster and the net charge it bears in the resting or other states remain controversial as discussed below. There are as yet really no synthetic systems that adequately model structure and function of the enzyme, although the capacity of abiological mononuclear Mo or W systems to convert dinitrogen to ammonia under ambient conditions is well established;[3, 7] chemical precedent for a carboxylate ligand functioning as a leaving group to unmask a dinitrogen binding site has been demonstrated,[8] and N–N bond cleavage reactions at dinuclear metal sulfur centres described.[9]

The M centre is ligated at the terminal Fe atom by a cysteinyl ligand and at the terminal Mo by a histidine ligand (Figure 1).[2] Rupturing this ligation allows extraction into *N*-methyl formamide (NMF) of the cofactor, FeMoco, which has the ability to restore nitrogen-fixing activity to a mutant protein devoid of the cluster.[10] Comparison between the EXAFS, EPR and Mössbauer spectroscopy of isolated FeMoco and that of the native protein, together with analytical data, indicate that the $\{Fe_7S_9Mo\}$ cluster core is conserved in the extracted cofactor and that it retains the chelating homocitrate ligand (Figure 2).[11]

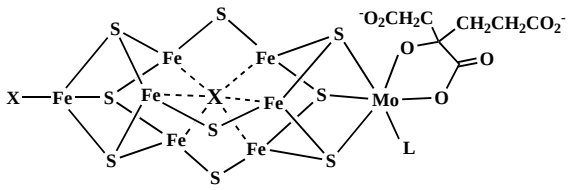

Figure 2. Schematic structure of isolated FeMoco. The interstitial light atom X is N (or possibly C or O) according to a recent high-resolution MoFe protein crystallographic analysis.[6]

Protocols for obtaining NMF solutions of FeMoco at ca. 1 mM concentration from the MoFe protein of nitrogenase in sufficient quantity are now well established. This has provided the opportunity for a wide range of direct chemical, spectroscopic, kinetic and electrochemical studies of the cofactor; these complement studies on the whole enzyme system and are beginning to provide some insights into how exogenous ligands, substrates and inhibitors interact with the isolated cluster.[12–15]

In this paper we describe aspects of the electrochemistry of FeMoco isolated from wild-type *Klebsiella pneumoniae* nitrogenase. Seminal work on the electrochemistry of FeMoco from *Azotobacter vinlandii* was described several years ago by Schultz and co-workers,[16] and we take their studies as our starting point. As expected from crystallographic data,[17] FeMoco isolated from either *K. pneumoniae* or *A. vinlandii* has indistiguishable spectroscopic and electrochemical properties.

Results and Discussion

Herein the $S = 3/2$ semireduced and EPR silent one-electron oxidised states of the extracted cofactor are abbreviated as FeMoco^{semired} and FeMoco^{ox}, respectively; other accessible redox states are correspondingly superscripted in the text. In the discussion, the corresponding states of FeMoco in the enzyme (the M centre) are designated M^{semired}, M^{ox} and so forth. In the text, successive reduction processes of FeMoco^{ox} are labelled **I**, **II**, and **III**, and electrochemical parameters such as the formal potential $E^{o\prime}$ and peak current i_p associated with these processes are accordingly superscripted, fop example, $^{\mathbf{I}}E^{o\prime}$.

The state of ligation of FeMoco: The protein cysteinyl and histidine ligands are de-coordinated from FeMoco when it is extracted from the protein into NMF. The question arises as to the nature of the exogenous ligands that coordinate to the terminal iron atom (Fe_{term}) and of those that occupy the capping Mo coordination sites of the isolated cofactor.

The terminal iron site: Earlier IR studies indicate that the *N*-deprotonated NMF anion ligates the terminal Fe atom,[18] whereas sulfur K X-ray absorption edge studies (XANES) have led to the proposal that Fe_{term} is ligated by a thiosulfate ligand.[19]

Figure 3 (lower trace) shows the cyclic voltammetric behaviour of FeMoco^{ox} in the potential domain which encompasses the primary reduction process that generates the FeMoco^{semired} system. The system displays two

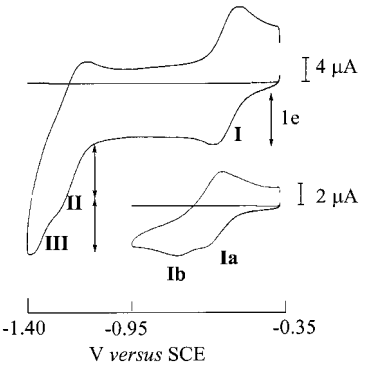

Figure 3. Lower trace: Cyclic voltammetry of a solution of FeMoco^{ox} in NMF at a vitreous carbon electrode recorded at 50 mV s^{-1} over a potential range encompassing the primary reduction process, showing two redox-dependent isomer forms of FeMoco$^{ox/semired}$. Upper trace: Primary and secondary reductions of FeMoco(SPh)^{ox} at 300 mV s^{-1}. The double-headed arrows represent one-electron currents based on $^{\mathbf{I}}i_{p\ red}$.

major redox active forms. The scan rate dependence of the voltammetry confirms that the redox couples are interconverted in dynamic equilibria as observed by Schultz and co-workers.[20] The difference in potential between the two redox couples is relatively small (90 mV); this is indicative of geometric or linkage isomerism rather than gross structural change. The structural integrity of the $\{Fe_7S_9Mo\}$ core upon extraction of the cofactor indicates that the redox isomerisation is associated with one or other of the exogenous ligand sites. The redox isomerism collapses when one equivalent of thiophenolate anion is added to the system and it is replaced by a single reversible one-electron process, with $E^{o\prime}$ close to that of the high-potential isomeric couple.[8, 12] Cysteine methyl ester similarly causes the collapse of the redox isomerism.

  0947-6539/03/0901-0077 $ 20.00+.50/0

The natural ligation of the Fe_{term} in the MoFe protein of nitrogenase is the thiolate group of a cysteinyl residue, and EXAFS studies of the isolated cofactor are concordant with thiolates similarly binding to Fe_{term}.[21] Clearly the loss of the redox-linked isomerism on addition of a thiol is directly related to the nature of the exogenous ligand at Fe_{term}. Thiolate coordination and substitution of the exogenous ligand at Fe_{term} leading to a single redox active form of the cofactor is paralleled by the sharpening of the broad EPR spectrum of FeMoco^{semired} upon the addition of thiols.[11] If the exogenous ligand binds in two different ways to Fe_{term}, then displacement of this ligand by thiolate will directly lead to the loss of isomerism. It will be shown below that this provides an explanation for the thiolate effect on the redox chemistry.

Replacing the exogenous ligand at Fe_{term} by thiophenolate has only a small effect on the redox potential of the primary FeMoco$^{ox/semired}$ couple; it is shifted approximately 30 mV positive relative to the primary redox potential of the isomer system. This can be set against observations obtained by Holm and co-workers on synthetic clusters:[22] replacement of a monodentate neutral ligand by an anionic ligand at the unique iron centre in site-differentiated Fe_4S_4 clusters that possess a tripodal thiolate ligand results in a large shift in the redox potential of the $\{Fe_4S_4\}^{3+/2+}$ couple to more negative values. For example, substituting the neutral ligands imidazole, 4-dimethylpyridine or tri-alkylphosphines by ethanethiolate shifts $E^{o\prime}$ potentials negative by more than 300 mV.[13] Thus the small positive shift of $E^{o\prime}$ observed upon replacing the exogenous ligand at Fe_{term} by an anionic thiolate ligand is inconsistent with substitution of a neutral donor ligand (for example, the solvent, NMF) by an anion. Rather, the shift suggests the substituted exogenous ligand is also anionic.

The redox-linked isomerism is associated with interconverting monodentate/bidentate ligation: Given that isomerism occurs at Fe_{term}, the question arises as to what type of anionic exogenous ligand might lead to the observed redox interconversions. Orme-Johnson and co-workers have reported solution and solid-film FTIR spectra of FeMoco^{semired} that are consistent with an N-bound anionic NMeCHO group ligating the cluster and have suggested that base-treated NMF is effective in extracting FeMoco from denatured protein, because the N-deprotonated form of the solvent coordinates to FeMoco as an anionic ligand (displacing cysteine).[18] We have shown that certain metal complexes with N-bound anionic amide ligands display two distinct redox couples with $E^{o\prime}$ values differing by about 120 mV.[23] This arises because two rotameric forms exist, one with the amide oxygen atom deployed towards the metal centre (amide ligand in the *cis* conformation) the other with it deployed away (*trans* amide conformation).[23] The significant activation energy for rotation about the N–C amide bond, approximately 20 kJ mol^{-1}, ensures interconversion of rotamers is relatively slow and thus allows observation of two redox couples at low temperature. As would be expected, the couple with the more negative redox potential has the oxygen atom deployed toward the metal centre (*cis* amide configuration), whilst that with the more positive E^{o} potential adopts the *trans* amide arrangement. The equilibrium distribution of the isomers depends upon the redox state of the complex with reduction favouring rotation of the donor oxygen atom away from the metal centre.[23]

The FeMoco$^{ox/semired}$ isomer system shows some parallel with this rotamer redox chemistry. Firstly, the difference in redox potential for the two FeMoco$^{ox/semired}$ isomers is about 90 mV. Secondly, the FeMoco^{semired} isomer with the more positive $E^{o\prime}$ is the more stable of the two forms (Figure 3). Thus one plausible interpretation of the electrochemical behaviour of FeMoco is that the exogenous anionic ligand bound at Fe_{term} is the amide anion $[NMeCHO]^-$,[18] with the redox isomerism arising from interconverting ligand *cis*–*trans* forms, as observed in the amide complexes (Scheme 1).

Set against this interpretation there is some dispute as to the necessity of using base-treated NMF to extract FeMoco.[24] Other solvents such as DMF can apparently be utilised provided that alkylammonium salts are present, although there are no published electrochemical data on FeMoco extracted in this fashion. Analysis by sulfur K-edge XANES has led to the suggestion that Fe_{term} is ligated by $[SSO_3]^{2-}$. The thiosulfate ligand is presumed to originate from the decomposition of dithionite ($[O_2SSO_2]^{2-}$), which is used to protect the cofactor from oxygen damage during its extraction from the MoFe protein.[19] Thiosulfate can behave as a mono- or bidentate ligand,[25] and, hence, there is the alternate possibility that redox isomerism is associated with interconverting η^1/η^2 coordination modes of thiosulfate rather than the suggested amide rotamerism.

Addition of $Na_2[SSO_3]$ has no effect on the cyclic voltammetry of FeMoco in NMF. Either thiosulfate does not displace an exogenous ligand at Fe_{term} or the exogenous ligand is thiosulfate. To test the propensity for thiosulfate to behave as a thiol ligand towards Fe atoms in synthetic clusters, we have examined its behaviour with $[Fe_4S_4Cl_4]^{2-}$. This cluster reacts rapidly and quantitatively with PhS^- in MeCN to give $[Fe_4S_4(SPh)_4]^{2-}$, a substitution that can be observed by cyclic voltammetry by the replacement of the $[Fe_4S_4Cl_4]^{2-/3-}$ couple by the $[Fe_4S_4(SPh)_4]^{2-/3-}$ couple which occurs at a more negative potential. In contrast, addition of an excess of $[NBu_4]_2[SSO_3]$ under the same conditions (vitreous carbon; MeCN 0.2 M, $[NBu_4][BF_4]$) leaves the $[Fe_4S_4Cl_4]^{2-/3-}$ couple unaffected and no new redox couple appears. Evidently thiosulfate moiety does not substitute chloride ligands in a synthetic cluster that possesses a similar Fe coordination environment to that of Fe_{term}. In contrast, Na[MeNCHO] does react with $[Fe_4S_4Cl_4]^{2-}$, although this leads to cluster degradation.[26]

We have also qualitatively examined the effect of acid and base on the native FeMoco system. We find that the redox-linked interconversion is not suppressed on treatment of the system with KO*t*Bu. As the acid concentration is enhanced, the potential of the second isomerism process is shifted to more positive values. This is fully consistent with shifting the equilibrium constants for the interconversion of the ox and red isomeric pairs towards the *trans,exo* C=O form; notably the redox equilibria of the model rotamer system are correspondingly sensitive to interactions of the *exo* carbonyl with solvent and ions, including protons.[23]

0947-6539/03/0901-0078 $ 20.00+.50/0 *Chem. Eur. J.* **2003**, *9*, No. 1

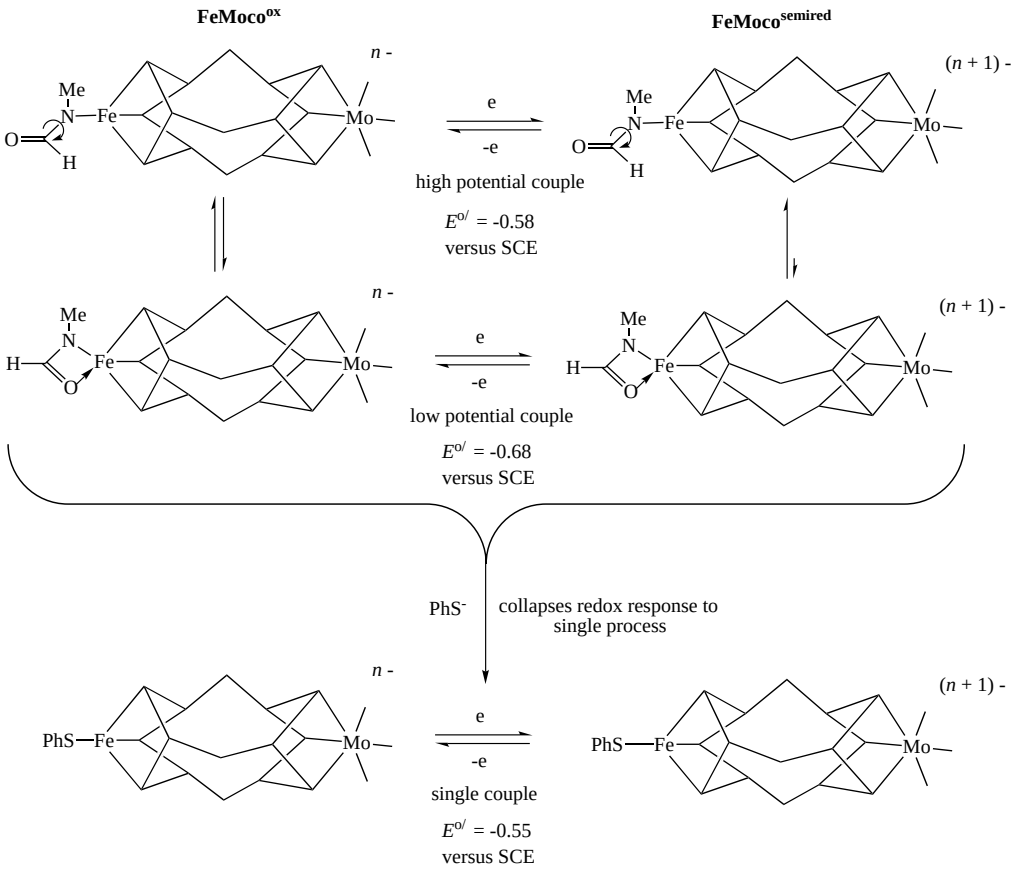

Scheme 1. Redox-linked isomerism at the terminal iron-site of FeMoco. The *cis* – *trans* isomerism of the *N*-methyl formamide ligand explains the occurrence of two redox processes with bidentate coordination disfavoured in the semireduced state.

In summary, redox isomerism at Fe_{term} is most likely associated with anionic NMF rather than thiosulfate, protic or other interactions.[27]

The molybdenum site: In the enzyme, the molybdenum atom of FeMoco is bound to the protein through a ligating donor ligand, histidine.[2] This is most likely replaced by a labile NMF ligand in the extracted cofactor. The coordination of other ligands to the molybdenum site of FeMoco have been studied by monitoring the kinetics of PhS^- substitution at Fe_{term} of $FeMoco^{semired}$.[28] Imidazole has only a minor effect on the kinetics of PhS^- substitution, consistent with replacement of NMF at the remote Mo site upon imidazole binding. Support for the binding of imidazole at Mo comes from comparison of analogous kinetic data for the native cofactor and that of $FeMoco^{semired}$ obtained from a $nifV^-$ mutant in which citrate rather than homocitrate is bound to Mo.[14, 29]

Reduced states of FeMoco: Figure 3 (upper trace) shows the well-defined cyclic voltammetry of the $FeMoco(SPh)^{ox/semired/red}$ electron-transfer series in NMF recorded at 300 $mV\,s^{-1}$. The peak current at fixed scan rate for the $FeMoco(SPh)^{ox/semired}$ couple ${}^{\mathbf{I}}i_p$ provides an internal one-electron standard for the *apparent* number of electrons transfered in other redox steps of FeMoco ($n_{apparent}$). Thus the ratio ${}^{\mathbf{II}}i_p/{}^{\mathbf{I}}i_p$ gives ${}^{\mathbf{II}}n_{apparent} = 1.1$ at 300 $mV\,s^{-1}$, consistent with two successive single-electron-transfer steps. The uncompensated peak-potential separations for the two successive reductions are essentially identical ($\Delta E = 70$ mV at 50 $mV\,s^{-1}$, 19 °C), again concordant with one-electron steps. As expected, at slower scan-rates ${}^{\mathbf{II}}n_{apparent}$ increases as the timescale allows reoxidation by protons at 50 $mV\,s^{-1}$, ${}^{\mathbf{II}}n_{apparent} = 1.5$; however, this does not affect the ratio ${}^{\mathbf{I}}i_p^{ox}/{}^{\mathbf{I}}i_p^{red} = 1.0$, because $FeMoco(SPh)^{semired}$ is regenerated.

There is a large separation of $\Delta E^{o\prime} = 630$ mV between the redox potentials for the $FeMoco(SPh)^{ox/semired}$ couple (Figure 3, process **I**) and $FeMoco(SPh)^{semired/red}$ couple (Figure 3, process **II**). Large values of ΔE are indicative of strong electronic interactions between redox orbitals as observed in synthetic cubane clusters.[30] The first and second FeMoco redox processes are consistent with successive addition of electrons to a delocalised cluster assembly (Scheme 2).

A hitherto unobserved third reduction, process **III**, is unmasked by thiophenolate modification of the cofactor, Figure 3. For the native cofactor, processes **II** and **III** are unresolved and at slow scan rates ${}^{\mathbf{II,III}}n_{apparent}$ becomes large as FeMoco engages in electrocatalysis of proton reduction to dihydrogen.[12] Thiophenolate coordination evidently shifts the redox potential of process **II** to a more positive value, thereby uncoupling the electrocatalysis (Figure 3). The value of ${}^{\mathbf{III}}n_{apparent}$ is 1.1 at 50 $mV\,s^{-1}$ and approximately 0.7 at 300 $mV\,s^{-1}$. The fact that reduction process **III** occurs at a potential less than 150 mV negative of process **II** shows that the redox orbital involved is insulated from the effect of

  0947-6539/03/0901-0079 $ 20.00+.50/0

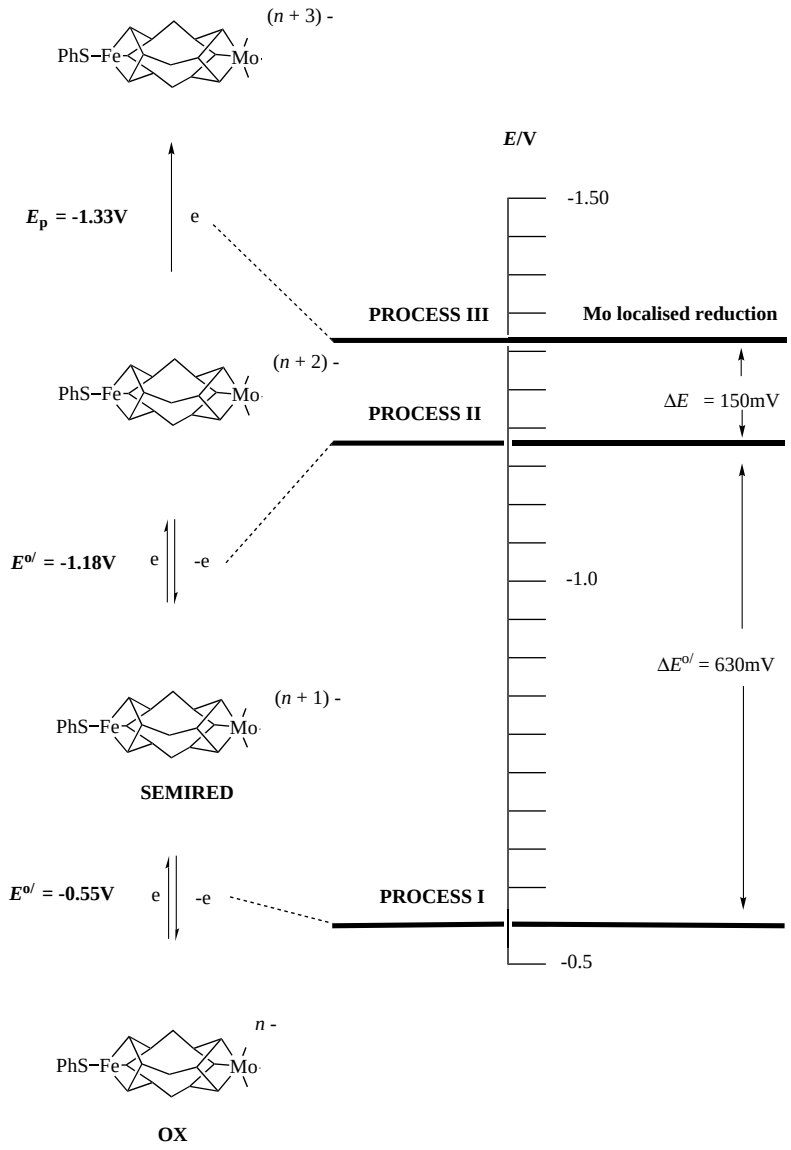

Scheme 2. Accessing reduced states of FeMoco. Processes **I** and **II** are separated by a large $^{I,II}\Delta E$ indicative of strongly interacting redox orbitals and are therefore associated with reduction of the iron core; the corresponding separation $^{II,III}\Delta E$ is relatively small consistent with process **III** being a localised Mo-centred reduction.

charge addition at the FeMoco(SPh)$^{semired/red}$ level. This is also consistent with the irreversibility of process **III** leaving the ratios $^{II}i_p^{ox}/^{II}i_p^{red}$ and $^{I}i_p^{ox}/^{I}i_p^{red}$ unperturbed. We therefore attribute **III** to a redox orbital localised on molybdenum (Scheme 2).

Imidazole is expected to coordinate to FeMoco in the same fashion as histidine in nitrogenase, that is, at the Mo site, and kinetic evidence for this has been discussed.[28, 29] Whereas the addition of one equivalent of thiophenolate has a dramatic effect on the electrochemistry of the native cofactor, stoichiometric concentrations of imidazole have no discernible effect on the overall cyclic voltammetry. At higher concentrations of the ligand (25 equivalents) the isomerism process at the FeMoco$^{ox/semired}$ level remains unaffected showing that imidazole does not bind at Fe_{term} at these oxidation levels to a measurable extent (Figure 4). However the subsequent reduction steps **II** and **III** are better resolved although both remain irreversible.

Hoffman and co-workers have assigned the oxidation states of the cofactor metal atoms in the semireduced ($S = 3/2$) form of the MoFe protein as {5Fe^{II}.(Fe^{III}–Fe^{II} pair).Mo^{IV}} on the basis of EPR and ENDOR studies of CO-modified forms.[31] This analysis is supported by a recent DFT study by Lovell et al.[32] If this assignment is correct, then reversibly generating the FeMoco(SPh)^{red} form of the cofactor would correspond to accessing an all-ferrous state with the further irreversible one-electron reduction generating a localised Mo^{III} level. However, Münck et al.[33] assign the formal oxidation states of M^{semired} as {4Fe^{II}.3Fe^{III}.Mo^{IV}} and this differs by two electrons from the earlier assignment.[31] In addition, these workers have also suggested that the generation of a Mo^{III} centre occurs during enzyme turnover on the basis of ^{57}Fe Mössbauer/rapid freeze data. They argue that the small difference of 0.02 mm s^{-1} for the isomer shift values, $\delta_{average}$, between the semireduced (M^{semired}) and an (integer spin) reduced state (M^{red}) indicates that an electron has been added to molybdenum on accessing the M^{red} (turnover) state. In contrast, radiolytic reduction of the MoFe protein in a synchrotron X-ray beam also generates an integer spin, reduced state which Münck et al. designate as M^{I}; however, in this case, reduction is thought to involve Fe rather than Mo.[33]

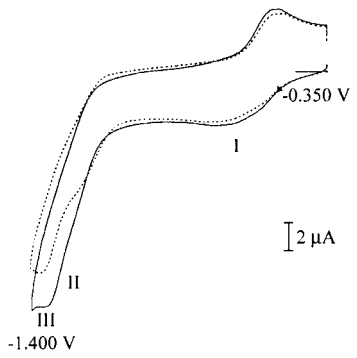

Figure 4. Cyclic voltammetry of FeMoco^{ox} at 50 mV s^{-1} (——); after addition of 75 molar equivalents of imidazole (••••).

0947-6539/03/0901-0080 $ 20.00+.50/0 *Chem. Eur. J.* **2003**, *9*, No. 1

The reductive electrochemistry of FeMoco(SPh)^{ox} is consistent with two successive electron transfers delocalised over the core iron–sulfur framework and a further localised reduction on the Mo centre. The relatively small difference in reduction potentials for accessing the FeMoco(SPh)^{red} and FeMoco(SPh)$^{red+1e}$ levels may have resonance with the observations on the protein by Münck et al.[33] that both iron and molybdenum based reductions are accessible.

The assignment of core iron and molybdenum localised reductions for the cofactor is further reinforced by the observation that processes **II** and **III** lead to the "independent" binding of carbon monoxide at two distinct types of redox site, as described below. The vexing question of oxidation states with the two-electron difference between assignments for M^{semired} as interpreted by the groups of Hoffman,[31] and Münck,[33] is addressed below in the light of the CO interactions with FeMoco.

Interaction of FeMoco with carbon monoxide: Dinitrogen, the natural substrate of nitrogenase is a π-acid ligand and can bind in a terminal fashion by σ donation to the metal and back donation from metal d orbitals into N_2 π* antibonding orbitals. We have examined the electrochemical/spectroelectrochemical response of FeMoco under argon and dinitrogen, but have been unable to detect any differences in behaviour of the systems at dinitrogen pressures up to 20 atm. This contrasts sharply with the considerable modification of the redox behaviour of FeMoco that is observed in the presence of carbon monoxide,[8] which has similar, but stronger, σ-donor/π-acceptor properties to that of terminally bound dinitrogen as now discussed.

Electrochemistry of FeMoco^{ox} under carbon monoxide: The primary reduction, process **I**, of the cofactor in its native or thiophenolate modified form is unaffected by CO. This is concordant with spectroscopic observations on the whole enzyme system, thus FTIR and EPR data show that CO does not bind to the resting state M^{semired} level of the native protein.[1, 34]

The key effect is observed on accessing the more reduced states: processes **II** and **III** become well resolved under CO at one atmosphere with $^{II}i_p$ substantially enhanced. Importantly, new product oxidation peaks are clearly evident, that is, processes **IV** and **V** in Figure 5a,b. Reversing the scan at −1.4 V gives rise to these peaks; holding at −1.4 V for several seconds prior to scan reversal leads to their build up and to a decrease of $^{III}i_p$ (Figure 5a,d). Peaks **IV** and **V** are not observed on reversal at −1.25 V unless the potential is first held for several seconds (Figure 5d,e). This observation is consistent with oxidation of CO-bound intermediates by protons until the concentration of H^+ is sufficiently depleted in the diffusion layer to allow detection of product species. Bulk electrolysis and FTIR spectroscopy experiments, which are discussed below support this interpretation.

One equivalent of thiophenol collapses the redox isomerism process to a single reversible one-electron response, as observed under dinitrogen, but otherwise has little effect on the voltammetry of FeMoco under CO (Figure 5b). Clearly, Fe_{term} is not involved in binding carbon monoxide. The

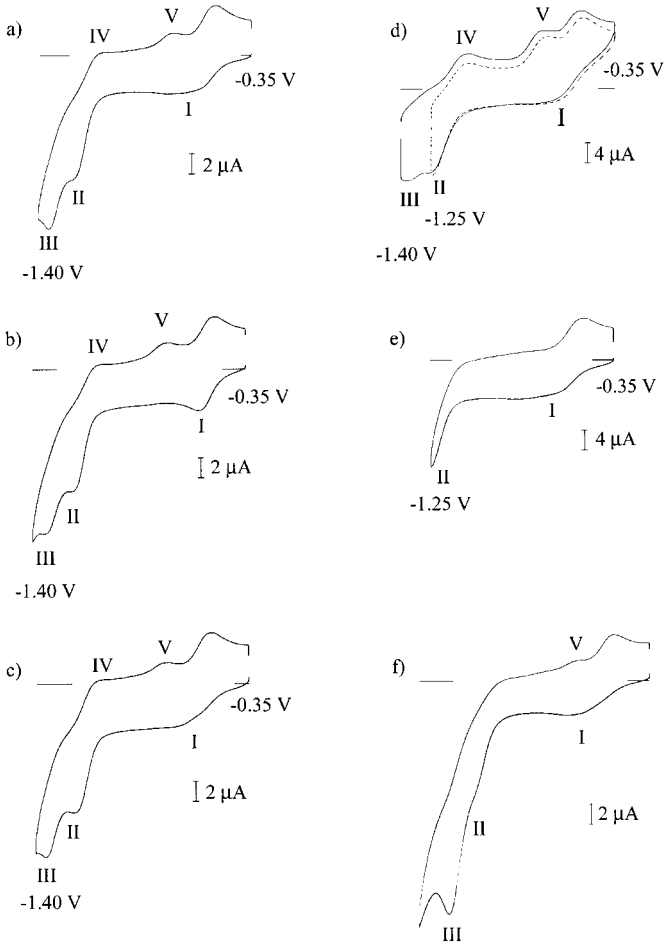

Figure 5. Cyclic voltammetry of FeMoco^{ox} after saturation of the NMF solution with CO at 1 atm, a) 50 mV s^{-1}; b) as for a) but after addition of 1 molar equivalent of thiophenol; c) as for a) but after addition of 75 molar equivalents of imidazole; d) 200 mV s^{-1} after holding the electrode at −1.40 V (——) or −1.25 V (••••); e) at 200 mV s^{-1} with a switching potential at −1.25 V. Scan f) was recorded at higher CO pressure, 19 atm at 50 mV s^{-1}.

thiophenolate-modified form provides for a comparison of the peak currents of steps **I** and **II**; from this it is evident that the latter approaches a two-electron-process under carbon monoxide (Figure 5b). At higher concentrations of thiophenol, catalysis of proton reduction competes with CO binding, processes **II** and **III** merge and the product peaks **IV** and **V** are suppressed (data not shown).

The effect of increasing the carbon monoxide concentration on the redox chemistry was probed by cyclic voltammetry under CO at about 19 atm. There is a dramatic enhancement of process **III** with a shift in $^{III}E_p$ to a more positive potential, consistent with fast following chemistry at high CO concentration (Figure 5f). The value of $^{III}n_{apparent}$ (50 mV s^{-1}) increases from 1.0 at 1 atm to 2.2 at 19 atm. Evidently at least four electrons can be transferred overall to FeMoco^{semired} at a moderate pressure of CO. The product peaks, processes **IV** and **V**, are suppressed, the significance of which becomes apparent below.

Imidazole at high concentration only marginally perturbs the cyclic voltammetry under CO. Small negative shifts in the

  0947-6539/03/0901-0081 $ 20.00+.50/0

oxidation potentials of process **III** and **V** and a slight positive shift in process **II** are observed (Figure 5c).

Controlled potential electrolysis on the thiophenolate modified cofactor was performed at -1.28 V under CO at 1 atm. The current decays in a four-phase fashion to about 40% of its initial value after the passage of approximately 4 F mol^{-1} of FeMoco^{ox}, and thereafter only slowly with increasing charge passed (Figure 6). In the initial phase a

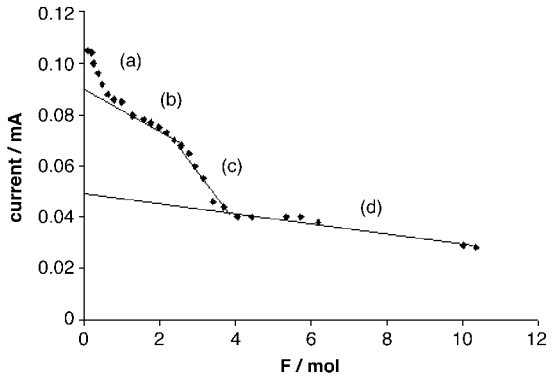

Figure 6. Controlled potential electrolysis of FeMoco^{ox} at vitreous carbon cathode held at -1.28 V versus SCE. The plot shows the cell current (constant stirring rate) versus the total charge passed.

the current rapidly decays towards a one-electron process consistent with bulk formation of FeMoco^{semired}. This is followed by a slower reduction phase b, which probably involves both proton turnover and CO binding at the FeMoco^{red} level until the acidity falls sufficiently for buildup of the three-electron-reduced carbonyl product, phase c, compare with Figure 5d,e. Slow reoxidation of the latter by protons would account for the observed plateau current in the final phase d. In support of this we find that interruption of the electrolysis after the passage of 4.5 F mol^{-1}, and examination by voltammetry, reveals the formation of the product associated with process **V** (Figure 7). However, the voltammetric product peak is not persistent and is lost after several seconds with reformation of FeMoco^{semired}.

In summary, these electrochemical results clearly show that carbon monoxide interacts with the cofactor on accessing

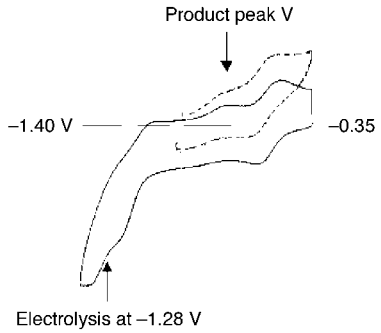

Figure 7. Cyclic voltammetry of the catholyte after reduction of FeMoco^{ox} showing formation of carbonyl species which gives rise to oxidation process **V**. The solid line shows the response before electrolysis, the broken line the response recorded immediately after passage of 4.5 F; the product peak **V** disappears after several seconds.

FeMoco^{red} and further reduced levels. Thus the initial interaction of CO with FeMoco^{red} leads to a second electron transfer that is reversible and occurs at a potential $E^{o\prime} = -1.05$ V (process **IV**), which is close to that of the FeMoco$^{semired/red}$ couple. At high CO concentration the enhanced current associated with process **III** is indicative of a further interaction with CO and also corresponds to the transfer of an additional electron (Figure 5d). Again it would appear that we are looking at electron-transfer chemistry associated with two essentially independent types of site, one associated with core iron atoms and the other associated with molybdenum, as we have observed in the absence of CO (compare with Scheme 2). Binding of CO at both types of site promotes further electron transfer, as is generally characteristic of reductive chemistry of transition metals under CO. Thus up to four electrons can be formally transferred to FeMoco^{semired} under moderate pressures of CO.

In order to more fully understand how CO interacts with reduced states of FeMoco we have investigated the FTIR spectroelectrochemistry of the system. This provides additional evidence that strongly supports reductive generation of two electronically distinct types of binding site associated with processes **II** and **III**. Importantly, it is shown that a bridging CO intermediate is formed at low CO conctration (Schemes 3 and 4).

FTIR thin-layer spectroelectrochemistry of FeMoco^{ox} under carbon monoxide: At low CO concentrations, FTIR spectroelectrochemistry encompassing reduction process **II** at about -1.2 V shows the generation of a CO-bound intermediate with ν(CO) at 1808 cm^{-1} (Figure 8a). This low-wavenumber, low-intensity absorption is attributed to the generation of a CO-bridged intermediate[35] on accessing FeMoco^{red} under CO limiting conditions (Scheme 3). Reoxidation at a potential more positive than that of process **IV** leads to the formation of an intermediate with ν(CO) at 1835 cm^{-1} (Figure 8a, Scheme 3). Importantly, it is possible to identify experimental conditions that confirm that the 1835 cm^{-1} band is generated as an intermediate following reduction of FeMoco^{semired} on the way to formation of the 1808 cm^{-1} band. Thus under lower CO concentrations and at short reduction time, a species with ν(CO) close to 1835 cm^{-1} is detected as an intermediate preceding the formation of the 1808 cm^{-1} species (Figure 8c), consistent with the initial binding of CO to FeMoco^{red} (Scheme 3). Thus we can associate process **IV** in the voltammetry under CO at 1 atm. with the one-electron redox interconversion of the bridged species and the irreversible process **V** with a further one-electron oxidation regenerating FeMoco^{semired}.

The difference $\Delta\nu$(CO) of about 30 cm^{-1} between the carbonyl bands of the one-electron redox-pair is evidently small. It has a parallel in the small values for $\Delta\nu$(CO) of approximately 20 cm^{-1} observed for both terminal and bridging ν(CO) upon successive one-electron addition to high-nuclearity platinum carbonyl clusters, as described by Dahl, Weaver et al.[36] in the context of the Stark effect.

At higher CO concentrations (7 atm CO) the 1808 cm^{-1} band is suppressed and intense absorptions are observed at 1920 cm^{-1} and 1885 cm^{-1}. This parallels the enhancement of

0947-6539/03/0901-0082 $ 20.00+.50/0 *Chem. Eur. J.* **2003**, *9*, No. 1

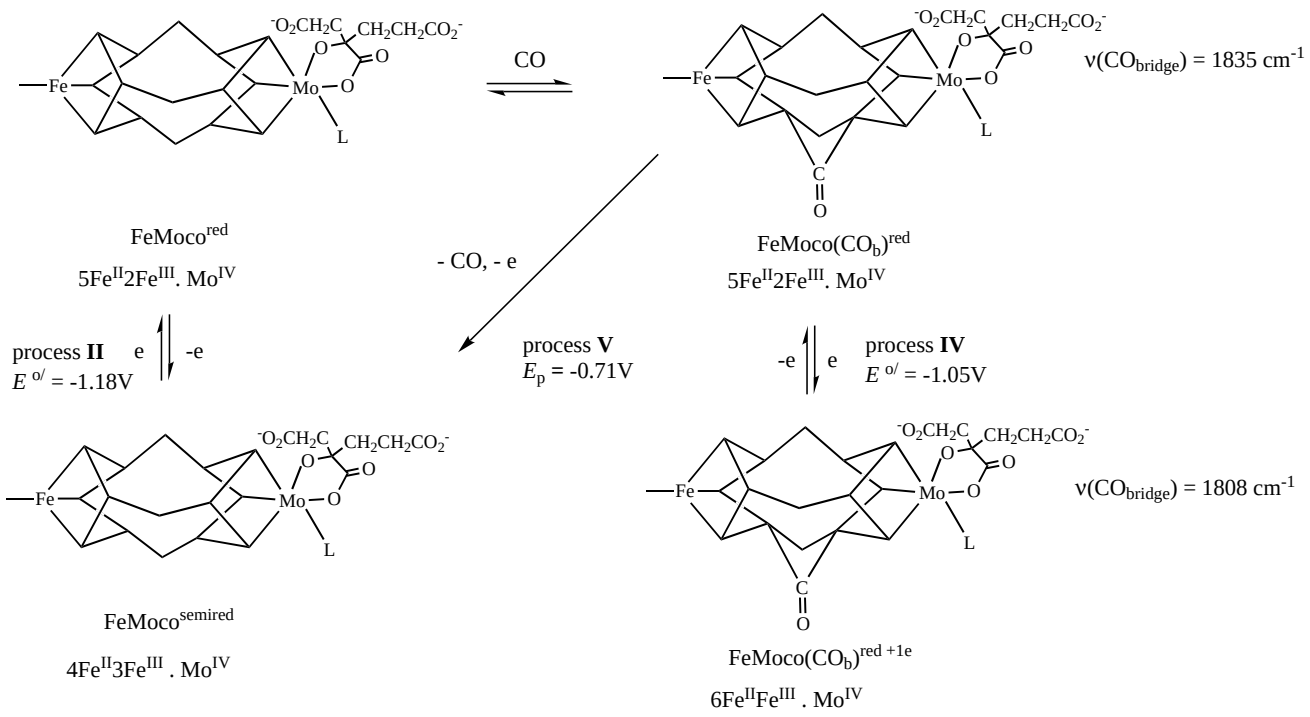

Scheme 3. Formation of bridged CO intermediates. Reduction of FeMoco that encompasses process **II** at low CO concentration leads to the formation of bridged CO intermediates, which are related by single-electron transfer.

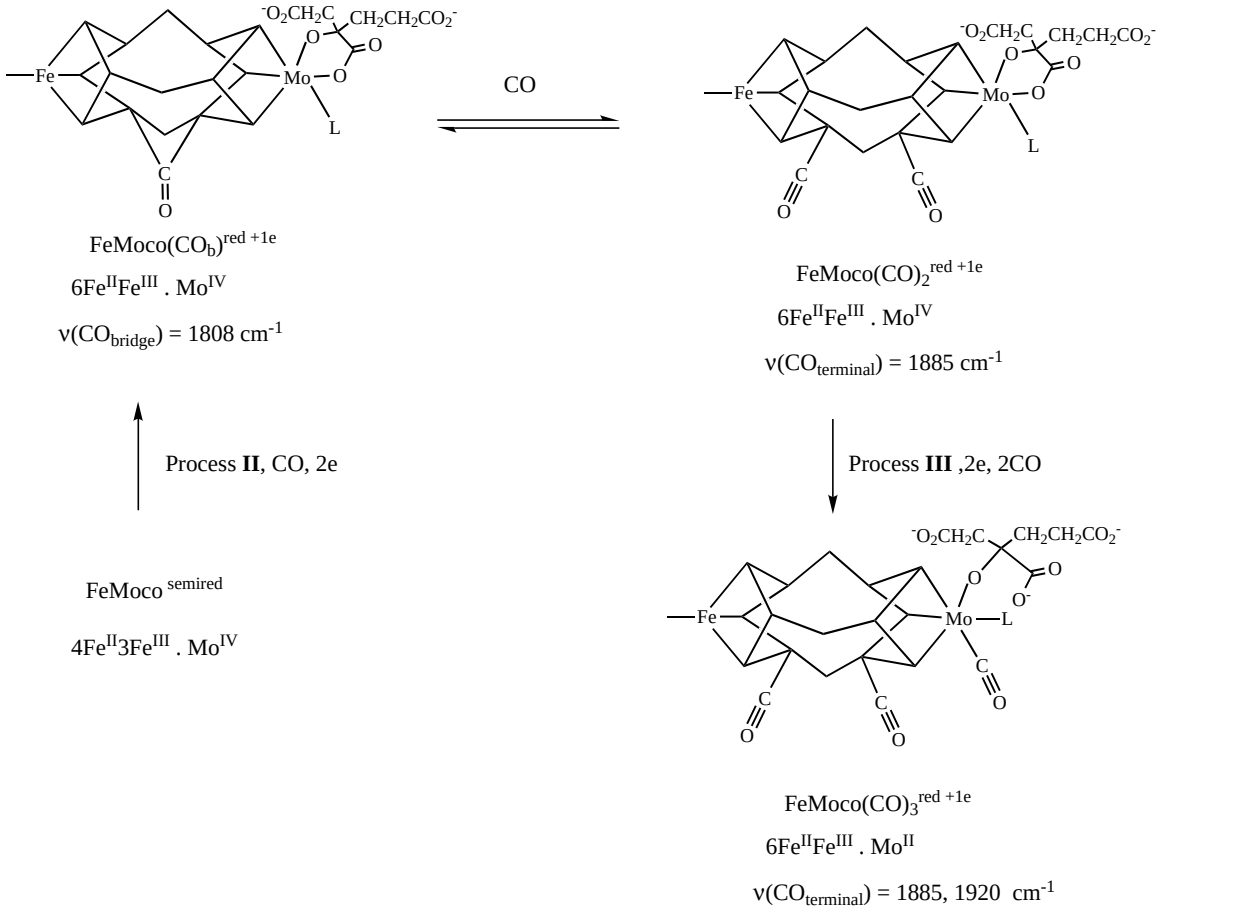

Scheme 4. The formation of 1species with terminal CO ligands. At high CO concentration, reduction that encompasses process **II** leads to the growth of a terminal CO band; reduction that encompasses process **III** leads to an additional band, which is vibrationally independent of that at the lower energy.

  0947-6539/03/0901-0083 $ 20.00+.50/0

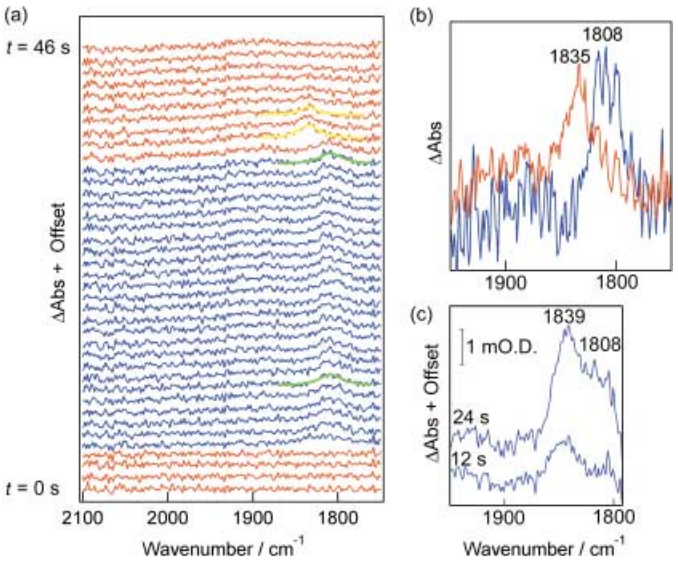

Figure 8. IR differential absorption spectra recorded during reduction and reoxidation of FeMoco^{ox} under a carbon monoxide atmosphere at 4 atm prior to equilibration of the gas in the NMF cofactor solution. In a), the single scans shown are recorded at 1.2 s time intervals from 0 to 46 seconds following application of potential steps from -0.35 V (red) to -1.2 V (blue) back to -0.35 V (red). Curves fitted to the ν(CO) bands in spectra recorded following the reduction step (green) and the reoxidation step (yellow) are superimposed on the original data. The band profiles from spectra recorded at about 10 s following the reduction and at 2.4 s following the reoxidation are expanded in b) to highlight the shift in wavenumber that accompanies reoxidation. The spectra in c) are averaged over 100 scans recorded at lower CO concentration (shorter equilibration time) at 12 s and at 24 s following a potential step from -0.35 to -1.2 V.

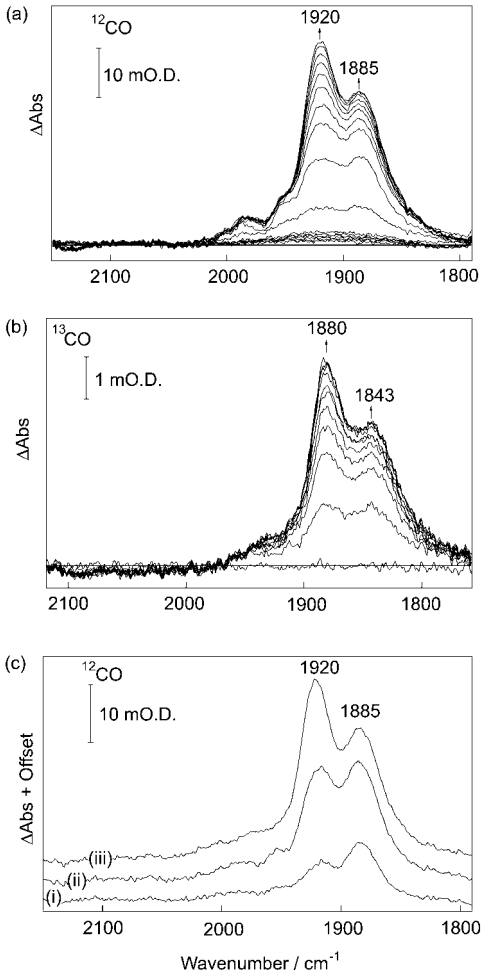

Figure 9. IR differential absorption spectra recorded following reduction of FeMoco^{ox} under a carbon monoxide atmosphere at 7 atm after equilibration of the gas in the NMF solution. Each spectrum is the average of 10 scans recorded over a period of 13 s: a) following reduction of FeMoco at -1.2 V; b) reduction at -1.4 V under ^{13}CO; c) at 60 s after switching the electrode potential to i) -1.0 V ii) -1.2 V and iii) -1.4 V.

process **III** in the voltammetry and the suppression of processes **IV** and **V** (Figure 5f). The broad band at 1885 cm^{-1} grows in first at -1.2 V (process **II**) and can be attributed to replacement of the CO bridge by terminal CO ligands (Figure 9a). At a potential of -1.4 V (process **III**) the 1920 cm^{-1} band grows in more rapidly, (Figure 9c). It is important to emphasise that the relative intensity of the bands change with time and potential with the *higher energy* band generated more rapidly at the *more negative* reduction potential. Furthermore, there is no significant transmission of electronic influence between the two types of centre: the growth of the 1920 cm^{-1} band does not perturb the position of the 1885 cm^{-1} band. This reinforces the interpretation that chemistry associated with process **II** ({6FeS7}-based) is essentially insulated from that involving process **III** (Mo-based). The results strongly support two independent types of CO binding site: one that is accessed under moderate CO pressures by reduction of the delocalised Fe core at the more positive potential giving rise to the 1885 cm^{-1} band, and one that is localised at the Mo centre and leads to the growth of the higher energy 1920 cm^{-1} band at the more negative potential (Scheme 4).

Thin-layer FTIR spectroelectrochemistry of FeMoco^{ox} under isotopically labelled ^{13}CO unambiguously confirms that bands observed under ^{12}CO (natural abundance) arise from carbon monoxide bound to reduced states of FeMoco. The bridging ^{12}CO band observed at 1808 cm^{-1} is shifted to 1778 cm^{-1} (calcd 1768 cm^{-1}) and the terminal bands at 1920 cm^{-1} and 1885 cm^{-1} are shifted to 1880 cm^{-1} (calcd 1878 cm^{-1}) and 1843 cm^{-1} (calcd 1843 cm^{-1}), as shown in Figure 9b.

Consistent with the cyclic voltammetry, the ν(CO) bands were unperturbed by generation of the thiophenolate form of the cofactor by addition of one equivalent of thiophenol. However, the binding of CO to the core Fe sites is inhibited by using excess PhSH as a weak proton source. In the presence of the thiol at 100 mM concentration the band at 1920 cm^{-1} rapidly develops, but that at 1885 cm^{-1} is suppressed (Figure 10a). If the potential is held for a prolonged period at -1.4 V then the proton concentration in the thin-layer cell is depleted and the 1885 cm^{-1} band increases in intensity (Figure 10a). This again emphasises the independence of the two types of site. The reason for suppression of the iron-based carbonyl band by protons must lie with a competition with CO for the reduced iron core site(s) and reoxidation of the reduced carbonyl species by protons (Scheme 4).

Figure 10b shows that the band that we associate with CO binding to molybdenum (CO binding to Fe suppressed by thiophenol) at 1920 cm^{-1} is split into two bands at 1930 and

0947-6539/03/0901-0084 $ 20.00+.50/0 *Chem. Eur. J.* **2003**, *9*, No. 1

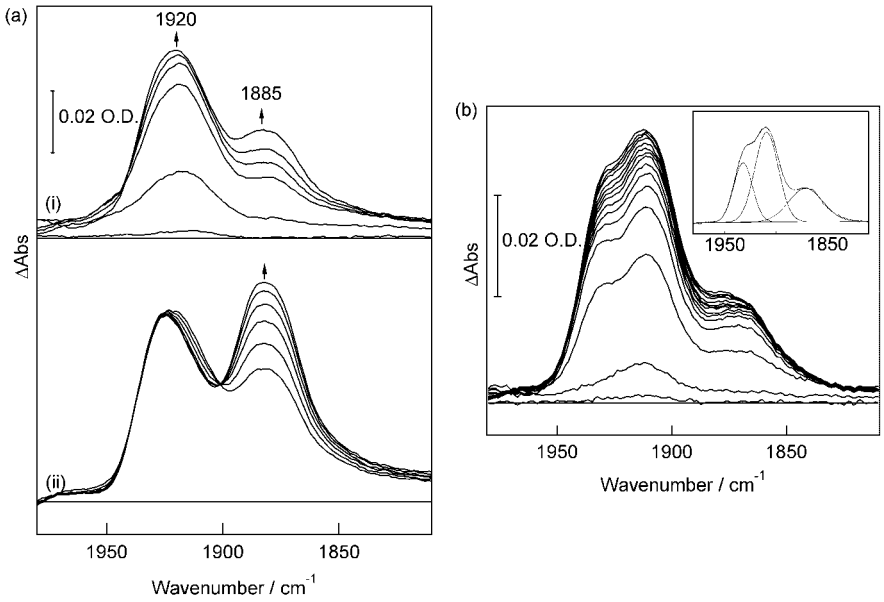

Figure 10. IR differential absorption spectra recorded under the same conditions as Figure 9; a) reduction of FeMoco at −1.4 V under a carbon monoxide atmosphere in the presence of a large excess of HSPh (>100 mM) over a period of i) 0–80 s and ii) 80–160 s following the potential step; conditions as for a), but after addition of a large excess of imidazole (ca. 50 mM), 0–160 s following reduction. The inset in b) shows a fit to the trace recorded at about 200 s following reduction (performed by using Grams-based routines implemented within BioRad WinIR software).

1910 cm^{-1} in the presence of imidazole at high concentration (50 mM). This may be explained by displacement of NMF at the Mo site by imidazole, for which two binding modes are possible: the electron donating ability of this ligand and hence the position of ν(CO) bands will depend on whether or not the $-CH_2CH_2COO^-$ arm of homocitrate forms hydrogen bonds with the imidazole NH group.[29]

Hoffman and co-workers have proposed, on the basis of EPR and ENDOR studies, that under turnover conditions the M centre of nitrogenase initially binds CO in a bridging mode between two iron atoms.[31] At higher carbon monoxide concentrations they propose that an additional CO binds to the M centre with a rearrangement to give a single terminal carbonyl ligand on two adjacent iron atoms. These results on the enzyme closely parallel those we have observed for the isolated cofactor when accessing the FeMoco^{red} level. Hoffman et al. suggest that the M centre in either the bridging or terminal CO-ligated states is at the same oxidation level as M^{semired}. Their argument for this is that CO bound to the M centre in terminal or bridging modes can be pumped off and this restores the spectroscopically well-defined EPR signal of M^{semired}.[31] Against this, however, is the observation that carbon monoxide will not directly bind to the resting state M^{semired} level. Our observations on FeMoco unequivocally show that the primary CO interaction with the cofactor requires accessing the FeMoco^{red} level. That M^{semired} is produced on removal of CO may be no more than a consequence of reoxidation of a more reduced level of the M centre by protons, which has a parallel with the instability of species detected under CO during bulk reduction of the isolated cofactor.

Taking the studies on isolated FeMoco and those on the M centre in the enzyme by Hoffmann, Münck and their co-workers together, we now suggest that the differing interpretation of redox states of M^{semired} can be rationalised by CO binding to iron atoms of the cofactor centre at a level two-electrons reduced from the semireduced level with M^{semired}. With the warning that an interstitial light atom may require revision of the interpretation of both Mössbauer and EPR/ENDOR results, we suggest that M^{semired} and FeMoco^{semired} are comprised nominally of the metal atoms in the redox states {4Fe^{II}.3Fe^{III}.Mo^{IV}}, as indicated in Schemes 2–4. Here we note that a synthetic trigonal-bipyramidal mononuclear Fe^{II}–monocarbonyl complex possessing a {Fe3SN} core has an ν(CO) band at 1885 cm^{-1} and that higher oxidation state Mo^{II} and Mo^{III} - carbonyls are not intrinsically unstable.[37, 38]

We have shown that the bridging carbonyl species detected at 1808 and 1835 cm^{-1} are related by a single-electron transfer. Oxidation of the terminally bound CO species can also lead to higher frequency ν(CO) modes. For example oxidation that encompasses process **V** leads to depletion of the 1885 cm^{-1} band and the growth of a new band at 1960 cm^{-1}. Stopped-flow FTIR studies of the binding of carbon monoxide to Mo–nitrogenase under turnover conditions have been reported.[34] At low CO concentrations a band at 1904 cm^{-1} is observed; at higher CO concentrations bands appear at 1958, 1936, 1906 and 1880 cm^{-1}. These bands broadly fall into the frequency range of our observations on FeMoco and are undoubtedly associated with terminal CO.

Conclusion

Here we summarise the main conclusions from this study.

1) Redox-linked isomerism is associated with the terminal (capping) iron site, and this probably involves monodentate/bidentate interconversion of *N*-methylformamide bound as an anion at Fe_{term}. Replacing this anion with PhS^- or other monodentate thiols switches off the isomerism (Scheme 1).
2) FeMoco(SPh)^{ox} undergoes two successive one-electron reduction processes the first of which is fully reversible at moderate scan rates, the second of which is reversible at fast scan rates. The magnitude of ΔE of 630 mV separating $^{II}E_p$ and $^{III}E_p$ of processes **I** and **II** is indicative of successive electron transfer to the delocalised {6FeS7} sub-cluster system.
3) A hitherto unrecognised further reduction process **III** is resolved by thiophenolate coordination at Fe_{term}. This

  0947-6539/03/0901-0085 $ 20.00+.50/0

irreversible electron transfer occurs at a potential close to that of $^{II}E_p$, indicative of a process localised at the Mo centre.

4) Reduction under carbon monoxide that encompasses process **II** at low CO concentration gives a bridging CO intermediate ($\nu(CO) = 1808\ cm^{-1}$), which reversibly oxidises in a one-electron step to give a bridging species with $\nu(CO) = 1835\ cm^{-1}$. At higher CO concentrations the bridging carbonyl species is converted to a product with terminally bound CO groups with $\nu(CO) = 1885\ cm^{-1}$. Given that process **II** is based on the {6FeS7} framework, CO interactions on accessing the FeMoco^{red} level are most likely, therefore, to involve binding to Fe. This is in parallel with the observations of Hoffmann that bridging and terminal binding of CO occurs between or at two neighbouring core Fe atoms during turnover of the enzyme.
5) Reduction under carbon monoxide that encompasses process **III** leads to the independent growth of a terminal CO band at $\nu(CO) = 1920\ cm^{-1}$ without measurable perturbation of the lower wavenumber band at $\nu(CO) = 1885\ cm^{-1}$. This shows that there is no vibrational coupling between the two types of CO binding centre and, importantly, there is no significant transmission of electronic influence between the two types of centre. This reinforces the interpretation that chemistry associated with process **II** ({6FeS7}-based) is essentially insulated from that involving process **III** (Mo-based).
6) Taking these studies on isolated FeMoco and those on the M centre in the enzyme by Hoffmann, Münck and their respective co-workers together, we suggest that the differing interpretation of redox states of M^{semired} can be rationalised by CO binding to iron atoms of the cofactor centre at a level two-electrons reduced from the semi-reduced level, with M^{semired} comprised nominally of the metal atoms in the redox states {4Fe^{II}.3Fe^{III}.Mo^{IV}}. It must be noted that no account is taken of an interstitial light atom in assigning this formalism. However, the interpretation of the isomer shifts obtained from Mössbauer measurements[34] is more straightforward if the central six iron atoms have distorted tetrahedral, rather than trigonal, coordination. Thus the revision of the structure strengthens the {4Fe^{II}.3Fe^{III}.Mo^{IV}} oxidation state assignment of M^{semired} and, hence, the conclusion that the high- and low-concentration CO forms are two-electron-reduced beyond M^{semired}.

Experimental Section

FeMoco preparation and assay: The nitrogenase MoFe protein was isolated from wild-type *K. pneumoniae* M5a1, and FeMoco was extracted into NMF containing water (ca. 2%), phosphate buffer and sodium dithionite, by using minor modifications of the methods described previously,[39] and concentrated in vacuo to about 1 mM (based on Mo determination, Southern Analytical, Brighton, UK). The integrity of isolated FeMoco was confirmed by C_2H_2 reduction activity in an enzyme reconstitution assay (activity >275 units mol^{-1} atom Mo), by EPR spectroscopy (Bruker ER 200 D-SRC, 4 K) and by cyclic voltammetry.

Materials: Imidazole and thiophenol (Aldrich) were used without further purification. NMF (Fluka) was distilled from anhydrous sodium carbonate and stored under N_2. Carbon monoxide and ^{13}CO (99.2 atom% ^{13}CO) were supplied by BOC (UK) and Trace Sciences International, Ontario (Canada), respectively.

Electrochemistry: Electrochemical measurements were performed by using a potentiostat Type DT 2101 and waveform generator PPRI (Hi-Tek Instruments, UK) and carried out in a glove box maintained at <1 ppm O_2 (Alvic Scientific Containment Systems, UK). The cell consisted of a small open vial fitted with a vitreous carbon working electrode (area 0.070 cm^2), a platinum wire auxiliary electrode and a saturated calomel reference electrode (SCE). The minimum working volume of the cell was 175 μL. The vitreous carbon electrode was polished with a 0.015 μm alumina slurry in ethanol prior to use.

High-pressure (19 atm) cyclic voltammetric measurements were made in a three-electrode cell contained within a Parr Instrument stainless steel bomb modified with electrical breakthroughs. All manipulations including filling the cell, assembly of the bomb, pressurisation and running of voltammograms were performed in the inert atmosphere glove box.

FTIR spectroelectrochemistry: The IR spectroelectrochemical cell was based on the standard absorption/reflection methodology, in which the interrogating radiation passes through the thin film of solution trapped between a transmitting window (CaF_2) and a highly polished working electrode.[40] The cell body was constructed so as to permit the application of moderate gas pressures (7 atm) to the solution under examination. Typically the thickness of the film of solution trapped between the vitreous carbon working electrode and the CaF_2 window was approximately 10–20 μm. Whereas vitreous carbon has about 50% of the reflectivity of platinum, the lower reflectivity of the former material is more than compensated for by its superior electrochemical properties, particularly its wider negative potential window. Platinum foil auxiliary and silver wire pseudoreference electrodes were contained within the sample space where a minimum volume of 50 μL was required to establish electrical contact between the three electrodes. Only a very small fraction of the bulk solution (ca. 0.1 μL) was subject to electrolysis at the working electrode in any one experiment allowing multiple experiments to be performed by exchanging the solution in the film. The FeMoco solution was transferred into the cell in a glove box and the cell transferred to the FTIR spectrometer (BioRad FTS60 and FTS 175C), where it was attached to the gas transfer lines. Equilibration of the gas and NMF phases in the cell without agitation took about 20 minutes. This allowed the qualitative effect of low concentrations of CO on the spectroelectrochemistry to be measured in the pre-equilibration period without compromising the integrity of cell by working at lower pressures.

Acknowledgement

We thank the BBSRC and the ARC for funding this work; the Bennett Fund for providing a travel scholarship to KAV; the ARC International Exchange Scheme (IREX) for providing travel funds to K.A.V., S.P.B. and C.J.P. and the John Innes and Leverhulme Foundations for Emeritus Fellowships to B.E.S. We also thank Dr S. A. Fairhurst for EPR characterisation of isolated FeMoco preparations.

[1] a) D. M. Lawson, B. E. Smith, *Met. Ions Biol. Syst*. **2002**, *39*, 75–119; b) B. K. Burgess, D. J. Lowe, *Chem. Rev.* **1996**, *96*, 2983–3011.
[2] a) J. Kim, D. C. Rees, *Science* **1992**, *257*, 1677–1682; b) J. B. Howard, D. C. Rees, *Chem. Rev.* **1996**, *96*, 2965–2982.
[3] C. J. Pickett, *J. Biol. Inorg. Chem.* **1996**, *1*, 601–606.
[4] a) D. Sellmann, J. Sutter, *J. Biol. Inorg. Chem.* **1996**, *1*, 587–593; b) D. Coucouvanis, *J. Biol. Inorg. Chem.* **1996**, *1*, 594–600.
[5] a) T. Lovell, J. Li, D. A. Case, *J. Am. Chem. Soc*. **2002**, *124*, 4546–4547; b) M. C. Durrant, *Biochem. J.* **2001**, *355*, 569–576; c) T. H. Rod, J. K. Norskov, *J. Am. Chem. Soc*. **2000**, *122*, 12751–12763; d) I. Dance, *J. Biol. Inorg. Chem.* **1996**, *1*, 581–586.
[6] O. Einsle, F. A. Tezcan, S. L. A. Andrade, B. Schmid, M. Yoshida, J. B. Howard, D. C. Rees, *Science* **2002**, *297*, 1696–1700.

[7] Y. Alias, S. K. Ibrahim, M. A. Queiros, A. Fonseca, J. Talarmin, F. Volant, C. J. Pickett, *J. Chem. Soc. Dalton Trans.* **1997**, 4807 – 4815.
[8] D. L. Hughes, S. K. Ibrahim, C. J. Pickett, G. Querne, A. Laouenan, J. Talarmin, M. A. Queiros, A. Fonseca, *Polyhedron* **1994**, *13*, 3341 – 3348.
[9] N. Le Grand, K. W. Muir, F. Y. Petillon, C. J. Pickett, P. Schollhammer, J. Talarmin, *Chem. Eur. J.* **2002**, *8*, 3115 – 3127.
[10] V. K. Shah, W. J. Brill, *Proc. Natl. Acad. Sci. USA* **1977**, *74*, 3249 – 3253.
[11] B. K. Burgess, *Chem. Rev.* **1990**, *90*, 2983 – 3011.
[12] T. Le Gall, S. K. Ibrahim, C. A. Gormal, B. E. Smith, C. J. Pickett, *Chem. Commun.* **1999**, 773 – 774.
[13] S. K. Ibrahim, K. Vincent, C. A. Gormal, B. E. Smith, S. P. Best, C. J. Pickett, *Chem. Commun*. **1999**, 1019 – 1020.
[14] B. E. Smith, M. C. Durrant, S. A. Fairhurst, C. A. Gormal, K. L. C. Grönberg, R. A. Henderson, S. K. Ibrahim, T. Le Gall, C. J. Pickett, *Coord. Chem. Rev.* **1999**, *185/186*, 669 – 687.
[15] M. A. Bazhenova, T. A. Bazhenova, G. N. Petrova, S. A. Mironova, *Kinet. Catal.* **2002**, *43*, 199 – 209.
[16] F. A. Schultz, S. F. Gheller, B. K. Burgess, S. Lough, W. E. Newton, *J. Am. Chem. Soc.* **1985**, *107*, 5364 – 5368.
[17] S. M. Mayer, D. M. Lawson, C. A. Gormal, S. M. Roe, B. E. Smith, *J. Mol. Biol.* **1999**, *292*, 871 – 891.
[18] M. A. Walters, S. K. Chapman, W. H. Orme-Johnson, *Polyhedron*, **1986**, *5*, 561 – 565.
[19] B. Hedman, P. Frank, S. F. Gheller, A. L. Roe, W. E. Newton, K. O. Hodgson, *J. Am. Chem. Soc.* **1988**, *110*, 3798 – 3805.
[20] W. E. Newton, S. F. Gheller, B. J. Feldman, W. R. Dunham, F. A. Schultz, *J. Biol. Chem.* **1989**, *264*, 1924 – 1927.
[21] I. Harvey, R. W. Strange, R. Schneider, C. A. Gormal, C. D. Garner, S. S. Hasnain, R. L. Richards, B. E. Smith, *Inorg. Chim. Acta* **1998**, *275 – 276*, 150 – 158.
[22] C. Y. Zhou, R. H. Holm, *Inorg. Chem*. **1997**, *36*, 4066 – 4077.
[23] M. C. Durrant, S. A. Fairhurst, D. L. Hughes, S. K. Ibrahim, M. Passos, A. Queiros, C. J. Pickett, *Chem. Commun*. **1997**, 2379 – 2380.
[24] S.-S. Yang, W.-H. Pan, G. D. Friesen, B. K. Burgess, J. L. Corbin, E. I. Stiefel, W. E. Newton, *J. Biol. Chem*. **1982**, *257*, 8042 – 8048.
[25] J. L. Burmeister, *Coord. Chem. Rev.* **1990**, *105*, 77 – 133.
[26] D. J. Evans, J. E. Barclay, personal communication.
[27] We thank a referee for drawing attention to the possibility that the redox interconversion might be a consequence of oligomerisation. [P. Frank, H. C. Angove, B. K. Burgess, K. O. Hodgson, *J. Biol. Inorg. Chem.* **2001**, *6*, 683 – 697.] However, the cyclic voltammetric response of the native cofactor as typified by Figure 3a fits well to a simulated scheme of squares for a one-electron redox-linked interconversion between isomeric forms. A similar voltammetric response can be simulated for monomer – dimer (first peak/second peak) redox-linked interconversion, but critically conversion to a single monomeric thiophenolate form is predicted to give a 35 % increase in the primary peak current for the isomerism and a 60 % increase for a monomer – dimer interconversion. Experimentally we find a 31 % increase, which is consistent with the former. Similar arguments obtain for higher "oligomeric" forms.
[28] K. L. C. Grönberg, C. A. Gormal, B. E. Smith, R. A. Henderson, *Chem. Commun.* **1997**, 713 – 714.
[29] K. L. C. Grönberg, C. A. Gormal, M. C. Durrant, B. E. Smith, R. A. Henderson, *J. Am. Chem. Soc.* **1998**, *120*, 10613 – 10621.
[30] C. J. Pickett, *Chem. Commun.* **1985**, 323 – 325. Separations of 700 – 1200 mV are typical of cubane clusters. For example, 1160 mV between the $[Fe_4S_4(SPh)_4]^{1-/2-}$ and $[Fe_4S_4(SPh)_4]^{2-/3-}$ couples and 860 mV between the $[Fe_4S_4(SPh)_4]^{2-/3-}$ and $[Fe_4S_4(SPh)_4]^{3-/4-}$ couples.
[31] H. I. Lee, B. J. Hales, B. M. Hoffman, *J. Am. Chem. Soc.* **1997**, *119*, 11395 – 11400.
[32] T. Lovell, J. Li, T. Liu, D. A. Case, L. Noodleman, *J. Am. Chem. Soc.* **2001**, *123*, 12392 – 12410.
[33] S. J. Yoo, H. C. Angove, V. Papaefthymiou, B. K. Burgess, E. Münck, *J. Am. Chem. Soc.* **2000**, *122*, 4926 – 4936.
[34] a) S. J. George, G. A. Ashby, C. W. Wharton, R. N. F. Thorneley, *J. Am. Chem. Soc.* **1997**, *119*, 6450 – 6451; b) R. N. F. Thorneley, S. J. George in *Prokaryotic Nitrogen Fixation: A Model System for Analysis of a Biological Process*, Horizon Scientific, Wymondham (UK), **2000**, pp. 1 – 19.
[35] K. Nakamoto, *Infrared and Raman Spectra of Inorganic and Coordination Compounds, Part B*, 5th ed., Wiley-Interscience, New York, **1997**, pp. 126 – 148.
[36] J. D. Roth, G. J. Lewis, L. K. Safford, X. Jiang, L. F. Dahl, M. J. Weaver, *J. Am. Chem. Soc.* **1992**, *114*, 6159 – 6169.
[37] S. C. Davies, D. L. Hughes, R. L. Richards, J. R. Sanders, *Chem. Commun*. **1998**, 2699 – 2700.
[38] B. A. L. Crichton, J. R. Dilworth, C. J. Pickett, J. C. Chatt, *J. Chem. Soc. Dalton Trans.* **1981**, 892 – 893.
[39] P. A. McLaine, D. A. Wink, S. K. Chapman, A. B. Hickman, D. M. McKillop, W. H. Orme-Johnson, *Biochemistry* **1989**, *28*, 9402 – 9406.
[40] a) S. P. Best, S. A. Ciniawsky, D. G. Humphrey, *J. Chem. Soc. Dalton Trans.* **1996**, 2945 – 2949; b) S. J. Borg, S. P. Best, *J. Electroanal. Chem.* in press.

Received: August 7, 2002 [F4325]

  0947-6539/03/0901-0087 $ 20.00+.50/0